Chin. J. Astron. Astrophys. Vol. 3 (2003), No. 4, 375–380
(http://www.chjaa.org or http://chjaa.bao.ac.cn)

Chinese Journal of
Astronomy and
Astrophysics

Near Real-Time Calculation of Ionospheric Electric Fields and Currents Using GEDAS

H. Shirai[1,2] ⋆, Y. Kamide[1], E. A. Kihn[3], B. Hausman[4], M. Shinohara[1,5], H. Nakata[1,6], M. Isowa[1], T. K. Takada[1], Y. Watanabe[1], and S. Masuda[1]

[1] Solar-Terrestrial Environment Laboratory, Nagoya University, Toyokawa, Aichi 442-8507, Japan
[2] Now at Ichinoseki National College of Technology, Ichinoseki, Iwate 021-8511, Japan
[3] NOAA National Geophysical Data Center, Boulder, Colorado 80303-3328, U.S.A.
[4] Department of Physics and Astronomy, Rice University, Houston, Texas 77005-1892, U.S.A.
[5] Now at Communications Research Laboratory, Koganei, Tokyo 184-8795, Japan
[6] Now at Chiba University, Chiba, Chiba 263-8522, Japan

Received 2003 March 4; accepted 2003 May 29

Abstract This paper presents the recent progress in our project of estimating near real-time electric fields and currents in the ionosphere through our computer system called the Geospace Environment Data Analysis System (GEDAS). We show a new technique in which data from ground magnetometers are collected by the system and used as input for the KRM and AMIE programs to calculate the distribution of ionospheric electric fields and currents, as well as of other ionospheric parameters, such as electric potential patterns. One of the goals of this project is to specify ionospheric processes. Examples of the near real-time calculation and the data flow of our scheme are presented.

Key words: data analysis — solar-terrestrial relations

1 INTRODUCTION

Calculation of ionospheric currents and fields in real time is essential to space weather research. In fact, forecasting/nowcasting techniques have been advanced greatly during the last decade. Two powerful tools have often been utilized for estimating ionospheric conditions. One is the so-called KRM method developed by Kamide et al. (1981). Using this technique, we can calculate two-dimensional distributions of ionospheric parameters over the entire polar region from ground magnetometer data. The other is the AMIE method (Richmond & Kamide 1988), in which ionospheric parameters are calculated by a statistical method of optimization. In this technique, many different types of measurement can be used, such as solar wind data from spacecraft, ground magnetometer data, and/or conductivities from radar. In this paper, we present a new technique to estimate ionospheric parameters in real time. This technique is an effective combination of the above two methods and is improved recently for the real time calculation. One of our projects is aimed at nowcasting/forecasting ionospheric parameters

⋆ E-mail: shirai@ichinoseki.ac.jp

on the basis primarily of ground-based magnetometer data from around the world through a newly installed computer system which is called the Geospace Environment Data Analysis System (GEDAS).

GEDAS was installed at the Solar-Terrestrial Environment Laboratory (STEL) for the following purposes (Kamide et al. 2001): 1. To make an integrated study of ground-based and spacecraft-based observations. 2. To efficiently connect data analysis and theory. 3. To construct algorithms for space weather predictions. Near real-time calculation of ionospheric parameters using GEDAS is one of the research projects to achieve these purposes. We now try to improve the entire scheme toward near real-time calculations by using both ground magnetometer data and spacecraft data.

2 CALCULATION

In our scheme, three algorithms are being utilized: KRM, rt-AMIE, and Local-KRM. The KRM algorithm calculates ionospheric electric fields and currents and field-aligned currents on the basis of ground magnetometer data (Kamide et al. 1981). It computes magnetic potential that is a best fit to the ground magnetometer data and then estimates electric potential patterns in the ionosphere using an ionospheric conductance model. The accuracy of the entire calculation process depends on, at least, three factors: the number of stations, numerical accuracies in determining electric and magnetic potentials, and the conductance model adopted in the scheme.

The rt-AMIE algorithm, standing for the real-time AMIE algorithm, is a simplified version of AMIE which is a technique to calculate ionospheric parameters from available information, such as ground magnetometer data and satellite observations of field-aligned currents (Richmond & Kamide 1988). The rt-AMIE algorithm that we employ is designed to use a statistical model of the electric potential (Weimer 1995). This potential pattern depends on solar wind conditions as measured by the ACE spacecraft (Zwickl et al. 1998).

Each of the KRM and rt-AMIE algorithms has its own advantages and certain disadvantages. Taking the strengths of each algorithm, we develope a new algorithm, which we call the local-KRM algorithm. Local-KRM is, in a sense, an effective combination of KRM and rt-AMIE. These two are used for separate estimates of ionospheric parameters for a local time sector where a number of stations are located (by KRM) and for the remaining sector with few stations (by rt-AMIE). For example, consider a case in which a number of stations exist in the local time sector of 12–23 MLTs, which we call sector A: see Figure 1c. Since the number of stations is large inside sector A, we are able to calculate the parameters in detail using the KRM algorithm. On the other hand, rt-AMIE, which relies on the empirical model of the electric potential, is suited for the remaining sector with only a few stations. After these separate calculations we combine the two types of output with great care to insure mathematical continuity at the boundary between the two local-time sectors.

At present, the number of stations providing real time data is between 10–50. Figures 1a, 1b, and 1c present examples of the electric potential calculated for 0240 UT of June 27, 2001 using KRM, rt-AMIE, and local-KRM, respectively. We have chosen this particular example for demonstration since this was at the maximum epoch of an intense substorm.

In the local-KRM calculation, we first use the rt-AMIE algorithm to calculate the global distributions of currents and electric potential. This part of the calculation is made at NOAA/NGDC. Once the global patterns are obtained, we calculate currents and electric potential for sector

A through KRM in the following way: (1) The difference is calculated between the magnetic field value expected from rt-AMIE and the value actually observed at each station within sector A. (2) The equivalent ionospheric current (IC) for this difference is estimated through KRM subject to the boundary condition that the difference is zero at the sector boundary. Therefore, the IC values calculated by KRM agree with those calculated through rt-AMIE at the boundary. (3) This estimated current is added to the current calculated through rt-AMIE. That is, we obtain the equivalent ionospheric current in sector A estimated through both rt-AMIE and KRM. Note that since the equations in our calculations are linear in terms of IC, separate calculations of IC are mathematically valid. Finally, the distribution of the electric potential in the ionosphere is derived from the distribution of IC using the ionospheric conductivity model of Ahn et al. (1998).

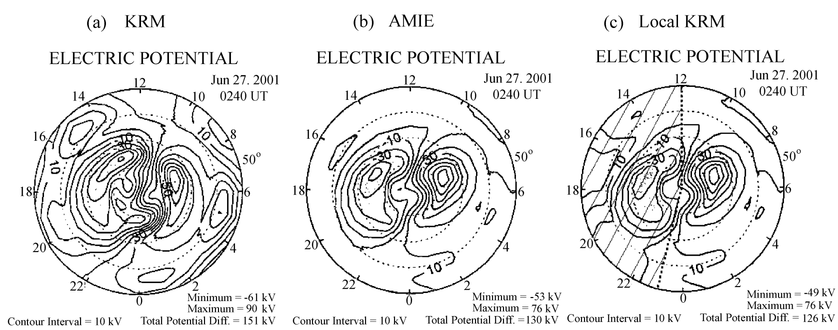

Fig. 1 Examples of near real-time calculations of the ionospheric electric potential using KRM (Fig. 1a), AMIE (Fig. 1b), and local-KRM (Fig. 1c). The 12–23 MLT sector, which we call sector A, is shown shaded in Fig. 1c.

Typical twin-vortex potential patterns can be identified in all the potential distributions in Fig. 1. The dusk-side potential pattern in the local-KRM output reflects both the KRM and rt-AMIE output, while the dawn-side pattern is a duplication of that of rt-AMIE. The total potential difference calculated by local-KRM is 126 kV, which is close to that in the AMIE output (130 kV), but is smaller than that in the KRM output (151 kV). This difference is attributable to an underestimate of the maximum potential on the dawn side resulting from a statistical model in the AMIE and local-KRM calculations and/or to an overestimate of the maximum potential value in the KRM calculation which is based on data from a small number of stations.

Figure 1c (the local-KRM output) also shows a large electric field on the dusk side, which is seen as a large potential difference in 16–18 MLT hours at latitudes of 55–75 degrees. The potential difference between a local maximum and minimum on the dusk sector is calculated to be about 70 kV at these local times. This structure is a direct reflection of large magnetic variations observed at the stations. A similar structure can be found also in the KRM output (Fig. 1a). The potential difference between the maximum and the minimum in 16–18 MLT hours is estimated as more than 70 kV. On the other hand, the rt-AMIE output (Fig. 1b) shows a smaller potential difference of about 50 kV on the dusk side. This means that the magnetometer data are not as strongly reflected in the rt-AMIE output as in the KRM and local-KRM output because of the use of a statistical electric potential model in rt-AMIE. It appears that the dusk-side pattern in the local-KRM output is a combination of the output from KRM and rt-AMIE.

3 DATA FLOW

Figure 2 presents a flow chart for data in the calculation scheme. First, ground magnetometer data and solar wind data from the ACE spacecraft are assembled at NOAA/NGDC. These data are being used for rt-AMIE. The rt-AMIE program outputs magnetic field data expected to be obtained on virtual stations arranged at certain intervals in the polar coordinate. Secondly, the rt-AMIE output (i.e., data from virtual stations) and the original ground magnetometer data are forwarded to GEDAS at STEL and are used as input for the local-KRM calculation. In this calculation, the magnetometer data, the AMIE output, and the KRM algorithm are combined. The local-KRM output includes equivalent currents, electric potential patterns, ionospheric currents, and field-aligned currents. The whole procedure, from ground-based observations to the local-KRM output, takes at present about 20–30 minutes, depending on the data transport and actual calculations.

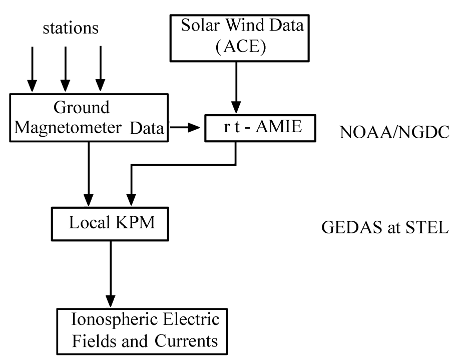

Fig. 2 Practical scheme for data flow and calculations. Ground magnetometer and solar wind data are assembled at NOAA/NGDC and are used as input for rt-AMIE. Output from rt-AMIE and the original ground magnetometer data are forwarded to GEDAS at STEL, where the local-KRM calculation is conducted.

4 NEAR REAL-TIME MONITORING

Figure 3 presents temporal variations of the electric potential patterns obtained for a period of five hours from 0240 UT of June 27, 2001, shown in Fig. 1. Although GEDAS is presently providing output distributions of ionospheric parameters every ten minutes, we show here only six distributions to survey overall variations. On this day, the IMF was directed southward (about minus 6 nT) until 0300 UT and then fluctuated around 0 nT. The corresponding geomagnetic activity was high at the beginning of this period, then decreased gradually, and became very quiet by 0740 UT. We see a twin vortex pattern in each of the potential distributions in Fig. 3. The total potential difference changed gradually. The total potential difference was near 124 kV until 0340 UT and then decreased to 55 kV by 0740 UT, suggesting that plasma

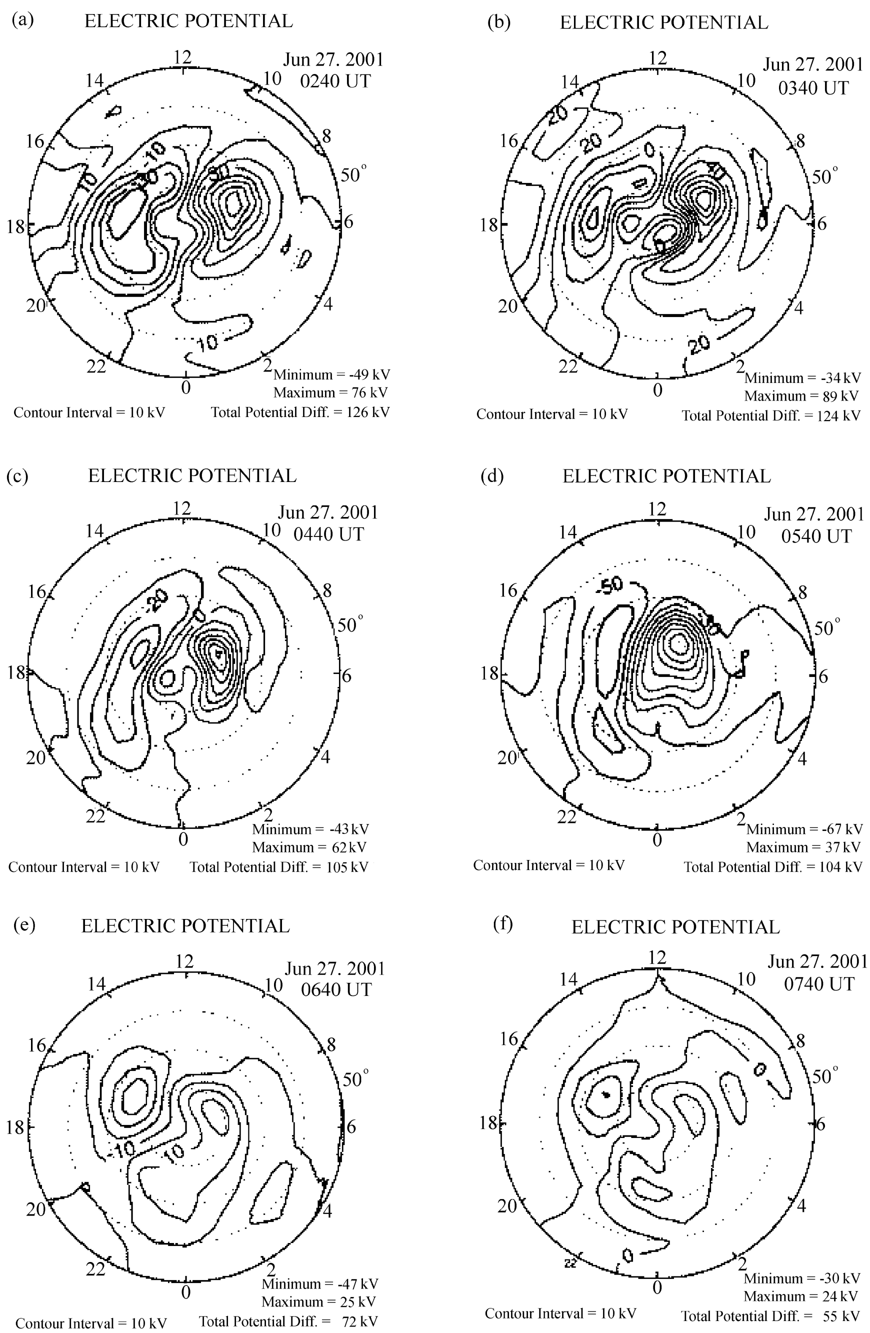

Fig. 3 Changes in the electric potential patterns calculated by the local-KRM program for (a) 0240, (b) 0340, (c) 0440, (d) 0540, (e) 0640, and (f) 0740 UT of June 27, 2001. The potential difference changed from 126 kV to 55 kV over the 5 hour period. This would be because the IMF Bz decreased gradually for this period and the magnetospheric plasma convection was weakened for the Bz decrease.

convection in the magnetosphere was weakened steadily due to the decrease in the magnitude of the southward component of the IMF. This series of potential distributions demonstrates clearly that we can discuss global patterns in the ionospheric electric potential and currents as well as magnetospheric convection in near real-time using the local-KRM technique.

It is also important to note that the local-KRM algorithm enables us to obtain smaller scale structures in a limited local time sector. These local structures in the ionospheric parameters result from magnetometer data from a number of stations in the sector. For example, we have seen in Figure 1c a local strong electric field (i.e., a large potential difference between the maximum and the minimum in 16–18 MLT hours at latitudes of 55–75 degrees). This electric field was weakened rapidly before 0440 UT, although the electric field on the dawn side remained strong until 0540 UT. It seems likely that the local-KRM technique is useful in discussing both global patterns and smaller scale structures in the distribution of ionospheric parameters.

5 DISCUSSION

In this paper, we have presented a new technique to estimate ionospheric parameters in near real-time through GEDAS, which was installed and developed recently at STEL. We can summarize our results in the following way. (1) A new technique, called local-KRM, represents an effective combination of two techniques: KRM and AMIE. (2) Using the local-KRM technique, it is possible to obtain the distribution of ionospheric parameters every 10 minutes or less on a real-time basis. (3) This new algorithm enables us to discuss both global and small scale structures in the patterns in ionospheric electric fields and currents, since the local-KRM method estimates the large-scale patterns over the entire polar region primarily from the AMIE technique and, at the same time, calculates the parameters in a limited local time sector with a higher accuracy by using data from a number of stations through the KRM technique.

We notice many advantages in our new method, but there seem to be some concerns regarding numerical issues. In this method, the polar region is divided into two local time sectors. One is the sector where a large number of stations exist, and the other is the remaining sector with few stations. In the example shown in Fig. 3a, the boundaries are located at the local times of 12 and 23 MLTs. These demarcation lines apparently rotate with the Earth, and are in fact 17 and 4 MLTs in Fig. 3f. In each panel, however, we find no significant discontinuity in the potential values at the boundaries. This indicates that assigning the boundaries does not create any artificial structures. We should also note that any structures seen in each panel do not rotate with the Earth. This also indicates that the potential patterns are not affected by the boundaries rotating with the Earth.

Acknowledgements We would like to thank the ACE team for providing solar wind data.

References

Ahn B.-H., Richmond A. D., Kamide Y., Kroehl H. W., Emery B. A., de la Beaujardiére O., Akasofu S.-I., 1998, J. Geophys. Res., 103, 14, 769
Kamide Y., Richmond A. D., Matsushita S., 1981, J. Geophys. Res., 86, 801
Kamide Y., Masuda S., Shirai H., Kim H.-J., Ogino T., Shinagawa H., Kojima M., Kihn E. A., Ridley A. J., 2001, Adv. Space Res., in press
Richmond A. D., Kamide Y., 1988, J. Geophys. Res., 93, 5741
Weimer D. R., J. Geophys. Res., 1995, 100, 19, 595
Zwickl R. D., Doggett K., Sahm S., Barrett B., Grubb R., et al., 1998, Space Sci. Rev., 86, 633